JOURNAL OF VIROLOGY, July 2003, p. 7756–7763 Vol. 77, No. 14
0022-538X/03/$08.00+0 DOI: 10.1128/JVI.77.14.7756–7763.2003
Copyright © 2003, American Society for Microbiology. All Rights Reserved.

Quantitative Analysis of Long-Term Virus-Specific CD8$^+$-T-Cell Memory in Mice Challenged with Unrelated Pathogens

Haiyan Liu,[1]† Samita Andreansky,[1] Gabriela Diaz,[1] Stephen J. Turner,[1] Dominik Wodarz,[2]‡ and Peter C. Doherty[1]*

Department of Immunology, St. Jude Children's Research Hospital, Memphis, Tennessee 38105,[1] and Program in Theoretical Biology, Institute for Advanced Study, Princeton, New Jersey 08540[2]

Received 11 October 2002/Accepted 22 April 2003

The consequences for the long-term maintenance of virus-specific CD8$^+$-T-cell memory have been analyzed experimentally for sequential respiratory infections with readily eliminated (influenza virus) and persistent (gammaherpesvirus 68 [γHV68]) pathogens. Sampling a broad range of tissue sites established that the numbers of CD8$^+$ T cells specific for the prominent influenza virus D^bNP_{366} epitope were reduced by about half in mice that had been challenged 100 days previously with γHV68, though the prior presence of a large CD8$^+$ $D^bNP_{366}{}^+$ population caused no selective defect in the γHV68-specific CD8$^+$ K^bp79^+ response. Conversely, mice that had been primed and boosted to generate substantial γHV68-specific CD8$^+$ D^bp56^+ populations did not show any decrease in prevalence for this set of CD8$^+$ memory cytotoxic T lymphocytes (CTL) at 200 days after respiratory exposure to an influenza A virus. However, in both experiments, the total magnitude of the CD8$^+$-T-cell pool was significantly diminished in those that had been infected with γHV68 and the influenza A virus. The broader implications of these findings, especially under conditions of repeated exposure to unrelated pathogens, are explored with a mathematical model which emphasizes that the immune effector and memory "phenome" is a function of the overall infection experience of the individual.

Our understanding of virus-specific CD8$^+$-T-cell-mediated immunity has been revolutionized over the past 5 years by the availability of tetrameric complexes of major histocompatibility complex class I glycoprotein plus peptide (tetramers) for the flow cytometric analysis of responder lymphocyte populations (2, 9). Prior to the advent of the tetramer technology, much of the extensive replication detected by propidium iodide staining of CD8$^+$ T cells recovered from the lymph nodes and spleen during the course of virus infections was thought to reflect the "bystander" activation of memory CD8$^+$ T cells specific for other antigens (29). This perception was based on estimates of virus-specific CD8$^+$-T-cell frequency determined by limiting-dilution analysis in 6-day microcultures (10). These limiting-dilution analysis values turned out, on average, to be at least 10-fold lower than the epitope-specific CD8$^+$-T-cell counts found with the tetramers (13, 20).

The extent of proliferation of tetramer$^+$ CD8$^+$ T cells can now be measured directly by giving infected mice the thymidine analogue bromodeoxyuridine in drinking water and then staining for the high-bromodeoxyuridine-expressing tetramer$^+$ CD8$^+$ set (14). With this approach, it can be formally shown that intercurrent infection with an unrelated virus does indeed induce some apparently unrelated CD8$^+$ memory T cells to cycle (3, 7) The extent of proliferation may, however, be three- to fourfold less than that observed for naïve or memory T cells responding to the inducing pathogen. This "bystander" effect has been variously attributed to unpredicted cross-reactivities (22) at the level of the clonotypic T-cell receptor and to induction by cytokines that operate via a final pathway involving interleukin-15 (26, 35).

The questions raised immediately by the very high CD8$^+$-T-cell frequencies (20) generated in, for example, mice infected with lymphocytic choriomeningitis virus included how there can be sufficient space within the immune system to accommodate the need to respond to a variety of pathogens and what the consequences are for immune homeostasis. One possibility that has been looked at is that bystander activation of established memory CD8$^+$-T-cell populations leads to the deletion of suboptimally activated lymphocytes (19, 22, 31). Another consideration is that there is some form of biological "sensor" that determines the overall magnitude of the CD8$^+$-T-cell pool. However, the size of the total CD8$^+$ set within a mouse can, at least for a time, be greatly expanded. This was shown very clearly for the murine gammaherpesvirus 68 (γHV68), which causes massive CD8$^+$-T-cell proliferation following respiratory challenge (11, 28).

The present experiments analyzed the extent to which established virus-specific CD8$^+$-T-cell memory to a prominent (13, 27) influenza A virus epitope (D^bNP_{366}) is modified by subsequent exposure to γHV68 and vice versa. There is no known cross-reactivity between these two viruses. Unlike previous studies that have addressed this question, the focus of our study was on the long-term consequences for immune memory.

MATERIALS AND METHODS

Mice and viral infection. Female, 8-week-old C57BL/6J (B6) mice (The Jackson Laboratory, Bar Harbor, Maine) were primed intraperitoneally with $10^{7.9}$ 50% egg infectious doses of the A/PR8/34 (PR8, H1N1) influenza A virus and

* Corresponding author. Mailing address: Department of Immunology, St. Jude Children's Research Hospital, 332 North Lauderdale, Memphis, TN 38105. Phone: (901) 495-3470. Fax: (901) 495-3107. E-mail: peter.doherty@stjude.org.

† Present address: University of Nevada School of Medicine, Reno, NV 89557.

‡ Present address: Fred Hutchinson Cancer Research Center, Seattle, WA 98109.

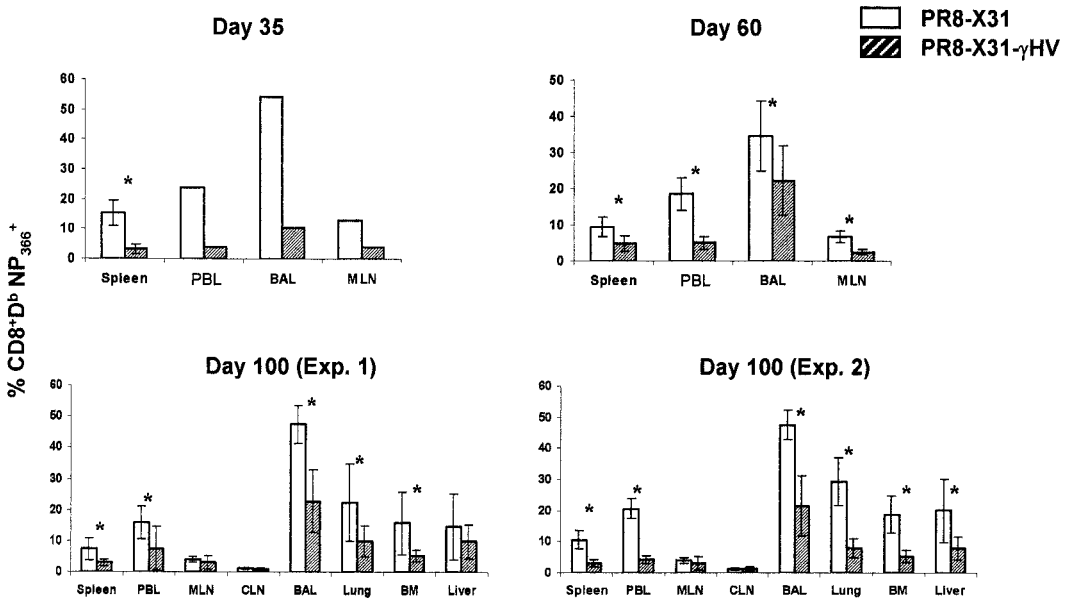

FIG. 1. Changes in the distribution of $CD8^+$ $D^bNP_{366}{}^+$ T cells at days 35, 60, and 100 after intranasal challenge of influenza virus-primed mice (PR8-X31) with murine γHV68 (PR8-X31-γHV). B6 mice were primed intraperitoneally with the PR8 influenza A virus (H1N1), boosted intranasally with the HKx31 (H3N2) virus, and then challenged intranasally with γHV68 (PR8-X31-γHV) or left unchallenged (PR8-X31) as described in the text. The interval between each virus treatment was 6 weeks, and the 35-, 60-, and 100-day time points are after the final γHV68 challenge. The bronchoalveolar lavage (BAL), peripheral blood lymphocyte (PBL), and mediastinal lymph node (MLN) populations from day 100 from two mice were pooled, and each data point shows the mean ± standard deviation for four samples (eight mice), while the spleens, lungs, livers, bone marrow (BM), and cervical lymph node (CLN) were analyzed from individual mice and each data point shows mean ± standard deviation for five mice. Otherwise, the results from day 35 and day 60 that show error bars are for five individuals, while the absence of error bars (day 35) indicates that the samples were pooled. The asterisk designates groups that were significantly different ($P < 0.05$).

then challenged intranasally with $10^{6.5}$ 50% egg infectious doses of the HKx31 (H3N2) virus (13) and later given 10^4 PFU of γHV68 intranasally (19). In a further study, naïve B6 mice were infected intranasally with γHV68, boosted intraperitoneally with 5×10^7 PFU of a recombinant vaccinia virus (Vacc-p56) incorporating the AGPHNDMEI p56 peptide (25), and then challenged intranasally with the HKx31 virus. The interval between sequential infections was 6 weeks in every case. In all experiments, naïve, age-matched controls were challenged with the final virus used.

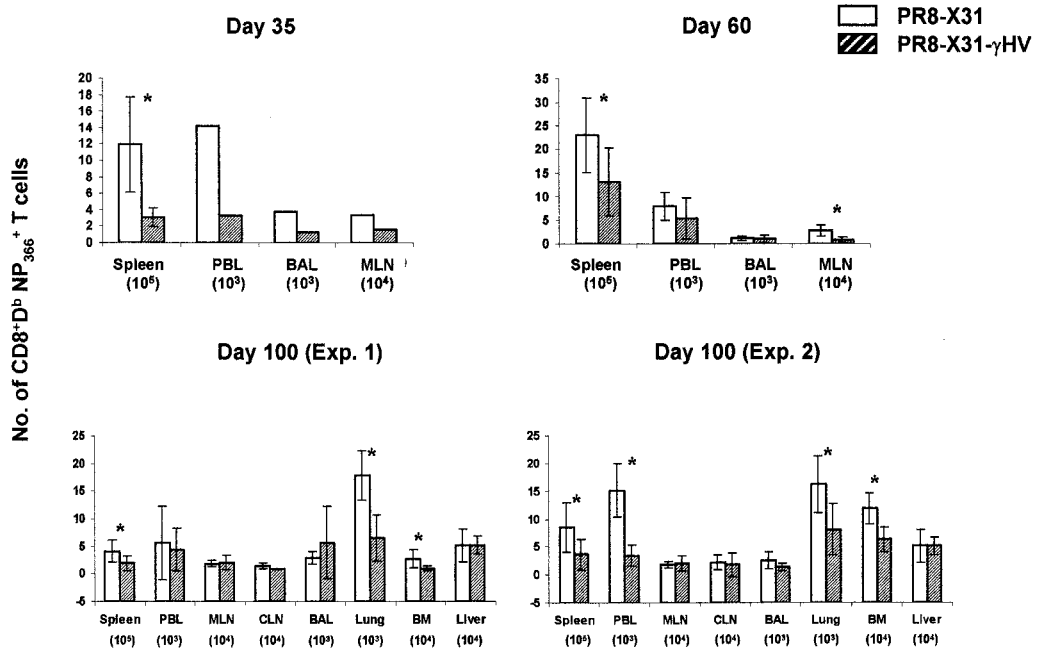

FIG. 2. Numbers of $D^bNP_{366}{}^+$ $CD8^+$ T cells per organ were calculated from the total $CD8^+$-T-cell counts and the values shown in Fig. 1. The asterisk designates groups that were significantly different ($P < 0.05$). See Fig. 1 legend for abbreviations.

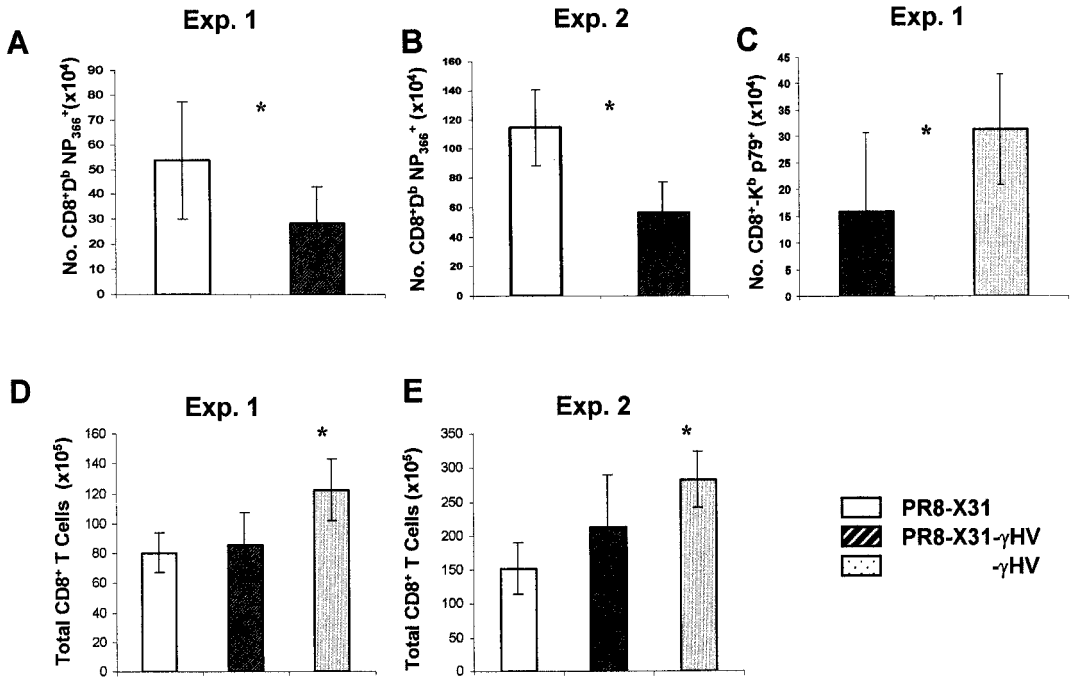

FIG. 3. Total counts (per mouse) for $CD8^+$ K^bp79^+, $CD8^+$ $D^bNP_{366}{}^+$ (A and B), $CD8^+$ $K^bp79^+CD8^+$ (C), and all $CD8^+$ T cells (panels D and E) were calculated for the day 100 (after γHV68) time point for the experiments shown in Fig. 1 to 4. The counts shown here were derived by summing the numbers per mouse for all the organs sampled. The spleens, lungs, livers, bone marrow, and cervical lymph node were analyzed from mice 1 to 5 of the eight sampled. The bronchoalveolar lavage, peripheral blood lymphocyte, and mediastinal lymph node samples were pooled for two mice (1 and 2, 3 and 4, 5 and 6, and 7 and 8). The numbers for the first three pools were halved and then added to the data for the other organs. The asterisk designates groups that were significantly different ($P < 0.04$).

Tissue sampling. The mice were anesthetized with Avertin (2,2,2-tribromoethanol; Sigma-Aldrich, St. Louis, Mo.) and bled from the right axillar artery (17). The blood was collected into heparinized phosphate-buffered saline (1,000 U/ml; Elkins-Sinn Inc., Cherry Hill, N.J.), and the inflammatory population was recovered from the pneumonic lung by bronchoalveolar lavage. Each mouse was then perfused with 40 to 60 ml of heparinized phosphate-buffered saline, and the lungs, mediastinal lymph nodes, cervical lymph nodes, livers, and spleens were removed. The bone marrow was flushed from the tibias and femurs with 5 to 10 ml of RP-10 medium (RPMI 1640 with 10% fetal calf serum), while the peripheral blood lymphocytes were separated on a 1-Step gradient (Accurate Chemicals, Westbury, N.Y.) by centrifugation for 30 min at 2,000 rpm. The cells were collected from the interface and washed, and the erythrocytes were lysed with ammonium chloride. The bronchoalveolar lavage populations were allowed to adhere to plastic for 1 h at 37°C to remove macrophages and monocytes.

Single-cell suspensions were made from the mediastinal lymph node, cervical lymph node, and spleen by grinding the tissues gently between glass slides. Lungs and livers were minced, forced through a fine stainless-steel mesh, filtered, and digested with collagenase (17). The bronchoalveolar lavage, peripheral blood lymphocyte, and mediastinal lymph node populations were pooled from two mice, while the spleens, lungs, livers, bone marrow, and cervical lymph nodes were analyzed from individual mice.

Flow cytometry. Spleen, cervical lymph node, and mediastinal lymph node populations were enriched for the $CD8^+$ set by in vitro depletion with monoclonal antibodies to $I\text{-}A^b$ (M5/114.15.2) and CD4 (GK1.5), followed by sheep anti-rat immunoglobulin and sheep anti-mouse immunoglobulin-coated magnetic beads (Dynal, Oslo, Norway). Virus-specific $CD8^+$ T cells were stained with phycoerythrin-labeled tetrameric complexes (13, 25) of $H\text{-}2D^b$ plus the influenza virus nucleoprotein ASNENMETM (D^bNP_{366}), the γHV68 p56 AGPHNDMEI peptide (D^bp56), or $H\text{-}2K^b$ plus the γHV68 p79 TSINFKVI peptide (K^bp79) at room temperature, followed by anti-CD8α-Tricolor (Caltag, South San Francisco, Calif.). Unenriched cells were also stained with anti-CD8α-fluorescein isothiocyanate and anti-CD4-phycoerythrin to determine the overall T-cell phenotype in the particular sample. The cells were stained and washed in ice-cold phosphate-buffered saline containing bovine serum albumin (0.1%) and azide (0.01%) and analyzed on a FACScan or FACScalibur with CellQuest software (Becton Dickinson, Mountain View, Calif.). The numbers presented in some of the figures were calculated from the total cell counts, the percent $CD8^+$, and the percent $CD8^+$ $tetramer^+$.

Mathematical modeling. The two basic variables in the mathematical model are the virus populations and memory CTL specific for each virus. It is assumed that a host can become infected with n different viruses. Virus of type i is denoted by v_i, and the memory CTL response specific to that virus is denoted by z_i, where $i = 1, 2, \ldots, n$. The model is given by the following set of differential equations:

$$\frac{dv_i}{dt} = r_i v_i\left(1 - \frac{v_i}{k_i}\right) - p_i v_i z_i \tag{1}$$

$$\frac{dz_i}{dt} = c_i v_i z_i - b_i z_i - z_i \sum_{j \neq i}^{j=1,2,\ldots,n} \alpha_j v_j \tag{2}$$

The virus replicates at a rate r_i. Replication is limited by the availability of susceptible host cells, which is captured in the parameter k_i. Virus replication is inhibited by the specific CTL response at a rate p_i. The memory CTL response becomes activated and proliferates in response to its specific antigen at a rate c_i. In the absence of antigen, the CTL response has an average life span of $1/b_i$. In addition, the model assumes that heterologous antigenic stimuli, v_j, reduce the memory CTL response to virus i (z_i) at a rate a_j. Thus, the model assumes the following mechanism for the reduction of memory CTL upon heterologous infection: heterologous antigen induces activation of the memory CTL through low-level cross-reactivity or bystander effects. Since the activation is induced by noncognate stimulation, these memory CTL do not go on to expand and increase significantly, but die (22, 31). Hence, the presence of the heterologous antigen is the force driving the reduction of CTL memory. An alternative idea would be that the CTL response to the heterologous infection competes with, and reduces, previously established memory. Such an assumption would, however, lead to the prediction that this new CTL response would also be selectively reduced if the existing memory pool is large.

When plotting the results of the model, it was assumed for simplicity that all infections have identical parameters. The qualitative outcome of the model does

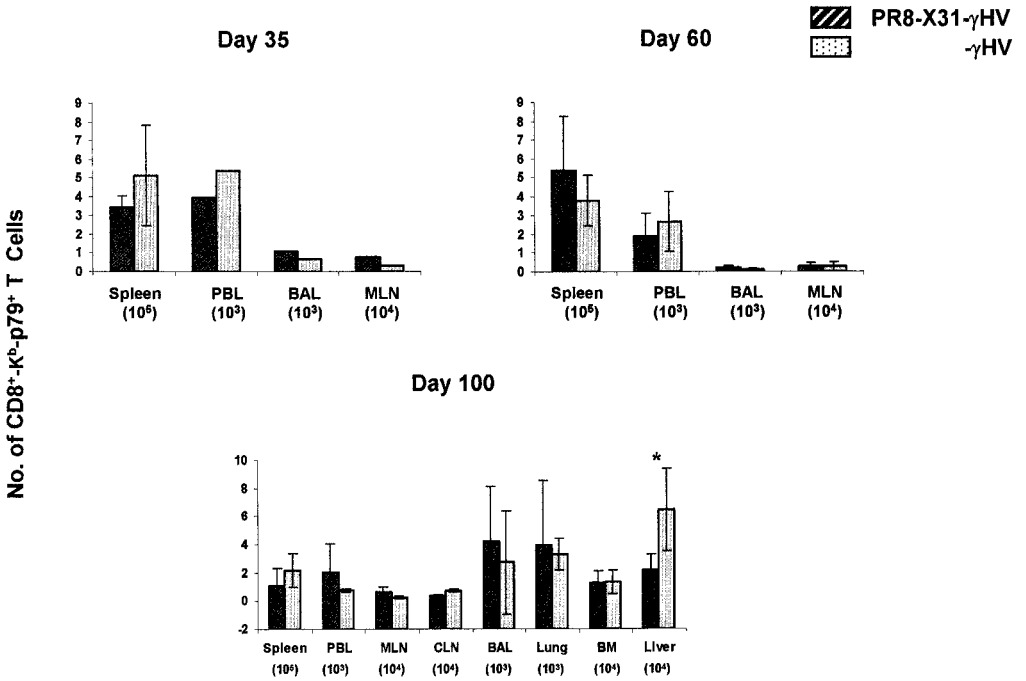

FIG. 4. Numbers of $CD8^+$ K^bp79^+ T cells are shown for the experiment described in the legend to Fig. 1. See Fig. 1 legend for abbreviations.

not, however, depend on this simplification. For a mathematically detailed analysis of the equations, see reference 32. The use of parameter values specific for the infections in question will require further experiments which would allow us to estimate the relevant parameters (presently unknown).

RESULTS

Challenging influenza virus-primed mice with γHV68. The C57BL/6J (B6) mice were first primed and boosted (13) with two different influenza A viruses (H3N2 and then H1N1) to give large numbers of $CD8^+$ $D^bNP_{366}{}^+$ T cells, rested for 6 weeks, and then challenged intranasally with γHV68 (6). The influenza viruses cause a transient, lytic infection that is substantially confined to the superficial epithelium of the trachea and lung and is generally resolved within 8 to 12 days (1, 8). There is no cross-neutralization (with antibody) between the H1N1 and H3N2 viruses, though both carry the $NP_{366\text{-}374}$ peptide that dominates the $CD8^+$-T-cell response (15). Respiratory exposure to γHV68 also induces a transient, lytic infection in lung epithelial cells (21, 23). However, this virus establishes latency in B cells and macrophages, and there is indirect evidence of sporadic reactivation to lytic phase for months after the initial encounter with the virus (3, 12, 34). In this respect it resembles other gammaherpesviruses, like Epstein-Barr virus (EBV), which can be detected routinely by PCR in the oropharynx of >30% of the human population (16).

Groups of at least five γHV68-challenged, H3N2- and H1N1-primed B6 mice (together with the appropriate controls) were sampled at 35, 60, and 100 days after the γHV68 challenge. At every time point tested, the $CD8^+$ $D^bNP_{366}{}^+$ T-cell frequencies were significantly reduced for the spleen, peripheral blood lymphocytes, and bone marrow recovered from those that had also been exposed to γHV68 (Fig. 1). This was also true for the lymphocytes that were isolated from the perfused, digested pneumonic lung (17) and for the inflammatory population that had first been removed by bronchoalveolar lavage. This pattern held up for the spleen, lung, and bone marrow when we calculated the numbers of $CD8^+$ $D^bNP_{366}{}^+$ T cells in each site (Fig. 2). Though the difference was not apparent for the draining mediastinal lymph node, cervical lymph node, bronchoalveolar lavage, and liver populations from those sampled on day 100 (Fig. 2), the total $CD8^+$ $D^bNP_{366}{}^+$ T-cell counts per mouse were approximately halved in the γHV68-infected, influenza virus-primed mice (Fig. 3A and B). The effect was selective, as estimates of the total $CD8^+$ lymphocyte count showed that there was no significant difference between the groups of influenza virus-immune mice that were and were not given γHV68 (Fig. 3D and E).

We also asked whether the presence of large, influenza virus-specific memory T-cell populations at the time of γHV68 challenge would modify the γHV68-specific response. Though the γHV68-specific $CD8^+$ D^bp56^+ set expands first after intranasal exposure to γHV68, this quickly gives way to $CD8^+$ K^bp79^+ T cells, which predominate in the long term (24). The only significant difference in $CD8^+$ K^bp79^+ T-cell numbers was found for the liver on day 100, when the counts were decreased for the mice that had first been exposed to the influenza A viruses (Fig. 4). Calculating the totals (per mouse) for $CD8^+$ K^bp79^+ T cells also showed that the value overall was significantly lower for the mice that had first been primed and boosted with the influenza A viruses (Fig. 3C). However, unlike the effect for the $CD8^+$ $D^bNP_{366}{}^+$ T cells (Fig. 3A, B, C, and D), this difference (Fig. 3C) was not specific for the $CD8^+$ K^bp79^+ set, as the total counts for all $CD8^+$ T cells were

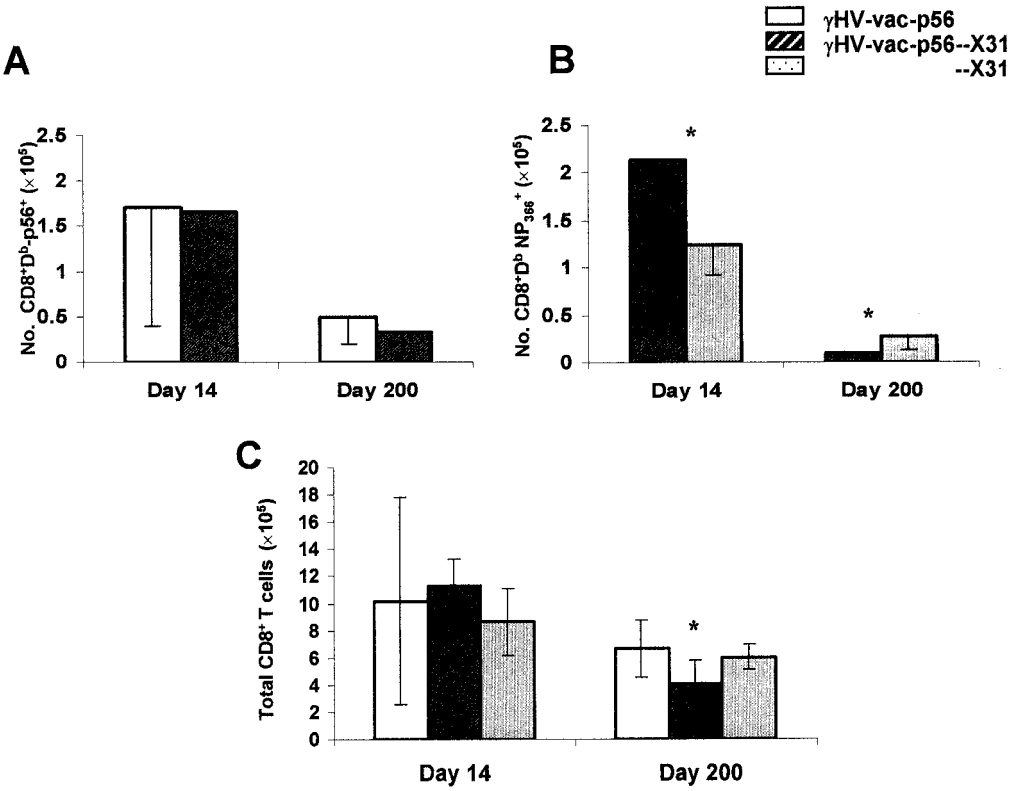

FIG. 5. Effect of influenza virus infection analyzed for spleen populations from mice primed with γHV68 and boosted to expand the $CD8^+$ K^bp56^+ population. The mice were given γHV68 intranasally, boosted intraperitoneally with Vacc-p56, and then (with age-matched, naïve controls) challenged intranasally with the HKx31 virus. The interval between each treatment was 6 weeks, and the mice were sampled 14 and 200 days after the influenza virus challenge. The number of $CD8^+$ D^bp56 (A), $CD8^+$ $D^bNP_{366}{}^+$ (B), and total $CD8^+$ (C) T cells was calculated and compared (mean ± standard deviation) for groups of five mice. The asterisk designates groups that were significantly different ($P < 0.05$).

significantly lower in the mice that were given both influenza virus and γHV68 (Fig. 3D).

Over the first 20 days or so after intranasal challenge with γHV68, the proliferation rate (measured by 6-day bromodeoxyuridine incorporation) of the $CD8^+$ D^bp56^+ and $CD8^+$ K^bp79^+ sets reached peak values of >85%, with evidence of cycling falling off more rapidly for the $CD8^+$ D^bp56^+ population (3). The $CD8^+$ D^bp56^+ T cells also turned over more slowly with elapsed time, supporting other indications that the lytic-phase K^bp79 epitope is present at higher levels in the long term. In fact, the $CD8^+$ K^bp79^+ set cycled at levels substantially above background for several months. During the acute phase of γHV68 infection (until day 16), an established $CD8^+$ $D^bNP_{366}{}^+$ T-cell population was also found to cycle at levels (18 to 20%) that were significantly above background (4 to 6%). The present findings establish beyond any doubt that this increased replication does not lead to augmentation of the $CD8^+$ $D^bNP_{366}{}^+$ memory T-cell pool and are in accord with findings from other experimental systems that the consequence of such bystander activation may be partial depletion of the memory T-cell pool (22).

Influenza virus pneumonia in mice with large numbers of $CD8^+$ D^bp56^+ T cells. Respiratory exposure to the HKx31 influenza A virus causes a substantial, nonfatal pneumonia, which generally starts to resolve within 14 days of infection (1). Memory T cells specific for unrelated antigens are readily detected in the population recovered by bronchoalveolar lavage (7, 29), and it is not clear whether such lymphocytes return to the recirculating pool or are lost to the host. Some increase in cycling is found for these "irrelevant" T cells (7).

Influenza virus challenge of mice that had been infected with γHV68 and then boosted with Vacc-p56 (4, 25) did not significantly modify the numbers of $CD8^+$ D^bp56^+ T cells recovered from the spleen 14 or 200 days later (Fig. 5A). Significantly more $CD8^+$ $D^bNP_{366}{}^+$ T cells were detected in the spleens of the γHV68-Vacc-p56 mice that were sampled on day 14, but the converse was true on day 200 (Fig. 5B). However, the total numbers of $CD8^+$ T cells in the spleen were also significantly reduced on day 200, though not on day 14 (Fig. 5C). In the present experiments, this did not lead to any decrease in the size of the established $CD8^+$ D^bp56^+ T-cell population in the spleen, though there is the caveat that the sporadic reactivation of γHV68 to lytic phase may have been associated with some degree of further antigenic stimulation. The effect of persistent if low-level γHV68 infection on T-cell turnover rates may also have had some influence on the significantly decreased numbers of both total $CD8^+$ and $CD8^+$ $D^bNP_{366}{}^+$ T cells on day 200 (Fig. 5).

DISCUSSION

The preceding experimental analysis (Fig. 1 to 5) shows what happens when there are two sequential infections. In nature,

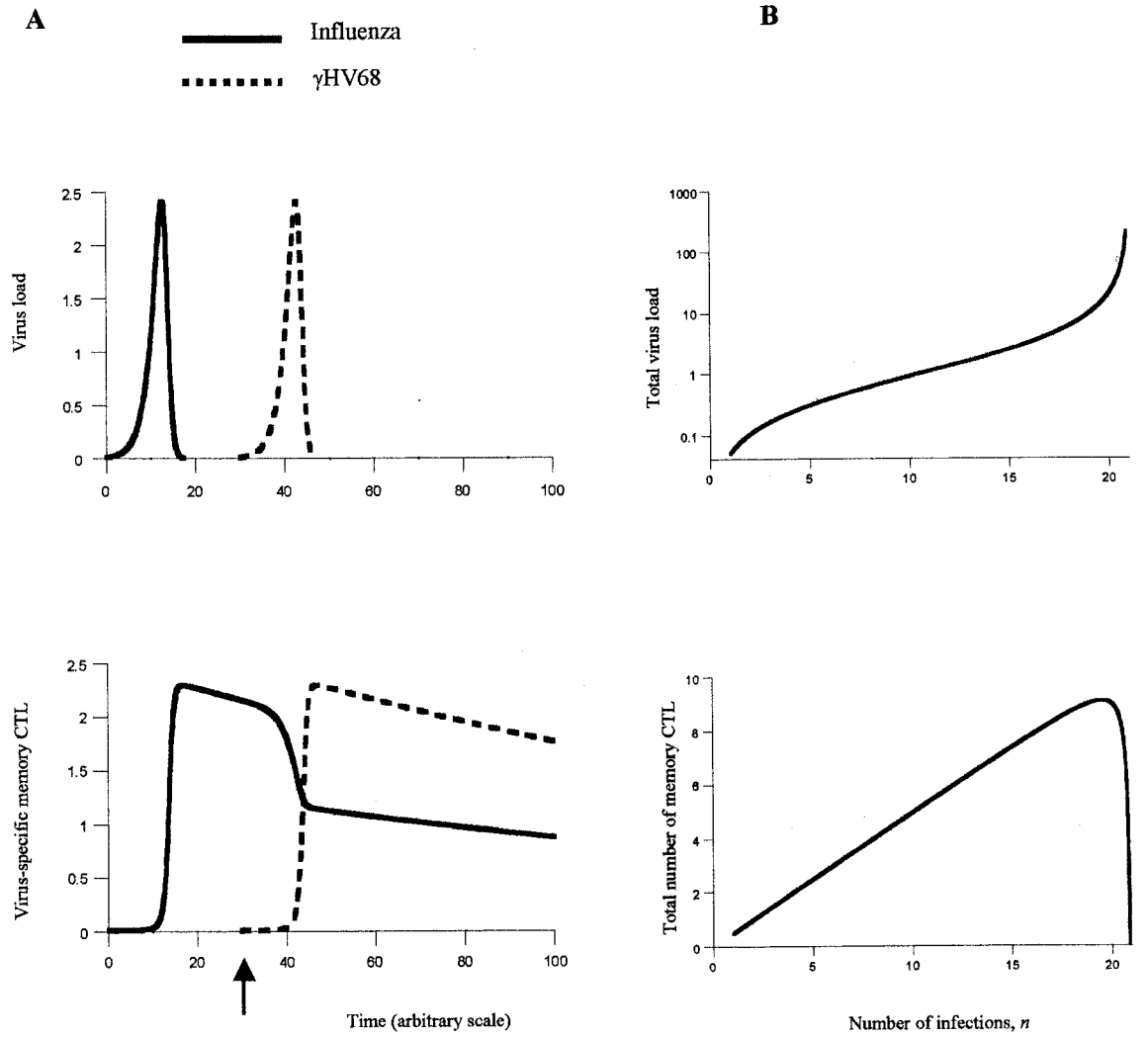

FIG. 6. Simulations according to the mathematical model. (A) Experiments (Fig. 1 to 4) in which mice were first primed with the influenza A virus and then challenged with γHV68. The arrow indicates the time of γHV68 infection. $r_i = 0.5$; $p_i = 1$; $k_i = 10$; $b_i = 0.005$; $c_i = 0.5$; $\alpha_i = 0.05$. For simplicity, parameters were assumed to be the same for both infections. (B) Extrapolation of the dynamics, assuming that a host is exposed to many pathogens. The graphs plot the total pathogen load and the total number of memory CTL summed over all infections as a function of the number of pathogens experienced by the host, n. The cumulative exposure weakens CTL memory generation against individual infections, with the potential consequence being the failure to clear the infectious agent. If the number of pathogens crosses a threshold, $n > (1/2)\ (1 + c/\alpha)$, the net consequence is an accelerated increase in overall pathogen load. This will result in a decline in the overall number of memory CTL summed over all infections if $n > (1 + c/\alpha) - \sqrt{kb(\alpha + c)}/ka$. The host becomes overwhelmed with pathogens and the CTL memory pool collapses if $n > (1 + c/\alpha) - b(c + \alpha)/cka$. These conditions allow us to obtain a qualitative understanding of the outcomes following cumulative exposure to pathogens. The stronger the CTL responses and the weaker the memory reduction induced by heterologous antigen, the greater the number of infections required to see these effects. Quantitative statements are not possible and are not the aim of this analysis, since the parameter values for all possible infections would have to be known. For simplicity, parameter values are assumed to be the same for all pathogens. Relaxation of this assumption leads to a qualitatively identical picture (33). Parameters were chosen as follows. $r_i = 0.5$; $p_i = 1$; $k_i = 10$; $b_i = 0.1$; $c_i = 2$; and $\alpha_i = 0.1$.

however, people are subject to many such events. We thus turned to a mathematical modeling approach for insight into how repeated exposure to pathogens might impact the establishment and maintenance of memory in the $CD8^+$ CTL compartment (32). The model assumes that the mechanism of CTL reduction is the activation of the memory CTL through low-level cross-reactivity or bystander effects induced by the heterologous antigen. The first step was to model the two-virus situation (Fig. 6A) that we analyzed experimentally (Fig. 1 to 4) in order to show that the mechanism underlying the model is consistent with observations. This simulation (Fig. 6A) does not, for simplicity, include any consideration of latency.

The model (Fig. 6A) starts with one infection which is resolved by a specific CTL response, corresponding to influenza virus in the experiment. After the virus is cleared, the memory CTL are long lived and decay only at a very slow rate. During this memory phase, a second virus (γHV68) is added to the system. The maximum virus load phase of lytic replication is resolved by the effector CTL response, leading to long-term CTL memory and control. During the time that the γHV68

load increases, the CTL memory response to influenza virus is reduced (Fig. 6A). As the γHV68 load is diminished, the CTL memory response against influenza virus is no longer negatively affected. The experimental data show that the CTL response against γHV68 is not selectively impaired (Fig. 3) despite the presence of high initial numbers of influenza virus-specific T cells. This is in accord with the model simulation, assuming that the heterologous antigen itself, and not CTL competition, is the reason for the reduction in CTL memory (Fig. 6A).

The two-virus situation (Fig. 6A) can then be extrapolated (Fig. 6B) to illustrate how such dynamics play out in the long term when a host is infected with a variety of pathogens over time. An obvious consequence is that established CTL memory to any given antigen will be successively diminished as more infections are experienced. Hence, the level of protection against secondary challenge will be concomitantly decreased. The consequences can, however, be more complicated. Some viruses, such as γHV68 and EBV, persist at low levels and are never eradicated. In addition, if several infections occur simultaneously or at close intervals, the model (Fig. 6B) suggests that a pathogen that might normally be cleared could become persistent, though held at low levels by a suboptimal response. At first, infections are readily controlled, and the total size of the antigen-specific CTL memory pool is relatively small. With the addition of further infection experiences, the overall pathogen load increases slightly and the total pool of memory CTL rises. If the number of infection events crosses a threshold, an accelerated loss of virus control will be seen with each sequential experience (Fig. 6B). When the number of infections increases further, the overall CTL memory pool will in fact decrease with every additional event. This decline can potentially lead to the collapse of all memory CTL. The net consequence would be that the host becomes overwhelmed with pathogens.

The experimental analysis thus illustrates what could occur following a de novo encounter (Fig. 1 to 4) with EBV (5) or when people who are carriers of EBV are infected with other pathogens (Fig. 5). This describes the situation for the majority of humanity, as almost every adult is an EBV carrier (33). The initial encounter with γHV68 causes massive $CD8^+$-T-cell proliferation (11, 28) that is in some senses similar to the infectious mononucleosis syndrome characteristic of primary EBV infection in adolescents (5). It is reassuring that the reduction in T-cell memory is, in both cases, only about twofold or less. This relatively subtle effect is not likely to have much impact on the capacity to develop an effective recall response.

However, extrapolating these effects with the mathematical model (Fig. 6) illustrates how the lifetime immune effector and memory "phenome" will be shaped by the overall antigenic (particularly the infection) history of the individual. The consequences for those in high-infection-load environments are potentially disastrous. Obvious example are people living in the developing world and those involved in high-risk behavior such as intravenous drug use. Such interactive effects need to be kept in mind as we attempt to develop effective vaccination strategies for these vulnerable populations. Furthermore, the model (Fig. 6) has important implications for antigenically variable pathogens (such as human immunodeficiency virus and hepatitis C virus) that expose the immune system to a wide variety of different antigenic stimuli over a relatively short time. This could result in the persistence of the virus variants, with overall virus load increasing as more antigenic strains are produced (32). When the number of antigenic strains crosses a threshold, CTL memory will decline and eventually collapse.

ACKNOWLEDGMENTS

This research was supported by USPHS grant AI29579, American Cancer Society grant PF-98-162-01 (S.A.), and the American-Lebanese-Syrian Associated Charities (ALSAC).

We thank Vicki Henderson for help with the manuscript and Mark Sangster for advice.

REFERENCES

1. **Allan, W., Z. Tabi, A. Cleary, and P. C. Doherty.** 1990. Cellular events in the lymph node and lung of mice with influenza virus. Consequences of depleting $CD4^+$ T cells. J. Immunol. **144:**3980–3986.
2. **Altman, J. D., P. A. Moss, P. J. Goulder, D. H. Barouch, M. G. McHeyzer-Williams, J. I. Bell, A. J. McMichael, and M. M. Davis.** 1996. Phenotypic analysis of antigen-specific T lymphocytes. Science **274:**94–96.
3. **Belz, G. T., and P. C. Doherty.** 2001. Virus-specific and bystander $CD8^+$ T-cell proliferation in the acute and persistent phases of a gammaherpesvirus infection. J. Virol. **75:**4435–4438.
4. **Belz, G. T, P. G. Stevenson, M. R. Castrucci, J. D. Altman, and P. C. Doherty.** 2000. Postexposure vaccination massively increases the prevalence of γ-herpesvirus-specific $CD8^+$ T cells but confers minimal survival advantage on CD4-deficient mice. Proc. Natl. Acad. Sci. USA **97:**2725–2730.
5. **Callan, M. F., N. Steven, P. Krausa, J. D. Wilson, P. A. Moss, G. M. Gillespie, J. I. Bell, A. B. Rickinson, and A. J. McMichael.** 1996. Large clonal expansions of $CD8^+$ T cells in acute infectious mononucleosis. Nat. Med. **2:**906–911.
6. **Cardin, R. D., J. W. Brooks, S. R. Sarawar, and P. C. Doherty.** 1996. Progressive loss of $CD8^+$ T-cell-mediated control of a γ-herpesvirus in the absence of $CD4^+$ T cells. J. Exp. Med. **184:**863–871.
7. **Christensen, J. P., P. C. Doherty, K. C. Branum, and J. M. Riberdy.** 2000. Profound protection against respiratory challenge with a lethal H7N7 influenza A virus by increasing the magnitude of $CD8^+$ T-cell memory. J. Virol. **74:**11690–11696.
8. **Doherty, P. C., J. W. Allan, M. Eichelberger, and S. R. Carding.** 1992. Roles of αβ and γδ T-cell subsets in viral immunity. Annu. Rev. Immunol. **10:**123–151.
9. **Doherty, P. C., and J. P. Christensen.** 2000. Accessing complexity: the dynamics of virus-specific T-cell responses. Annu. Rev. Immunol. **18:**561–592.
10. **Doherty, P. C., D. J. Topham, and R. A. Tripp.** 1996. Establishment and persistence of virus-specific $CD4^+$ and $CD8^+$ T-cell memory. Immunol. Rev. **150:**23–44.
11. **Doherty, P. C., A. M. Hamilton-Easton, D. J. Topham, J. Riberdy, J. W. Brooks, and R. D. Cardin.** 1997. Consequences of viral infections for lymphocyte compartmentalization and homeostasis. Semin. Immunol. **9:**365–373.
12. **Flano, E., Woodland, D. L., M. A. Blackman, and P. C. Doherty, P. C.** 2001. Analysis of virus-specific $CD4^+$ T cells during long-term gammaherpesvirus infection. J. Virol. **75:**7744–7748.
13. **Flynn, K. J., G. T. Belz, J. D. Altman, R. Ahmed, D. L. Woodland, and P. C. Doherty.** 1998. Virus-specific $CD8^+$ T cells in primary and secondary influenza virus pneumonia. Immunity **8:**683–691.
14. **Flynn, K. J., J. M. Riberdy, J. P. Christensen, J. D. Altman, and P. C. Doherty.** 1999. In vivo proliferation of naive and memory influenza virus-specific $CD8^+$ T cells. Proc. Natl. Acad. Sci. USA **96:**8597–8602.
15. **Kilbourne, E. D.** 1969. Future influenza virus vaccines and the use of genetic recombinants. Bull. W. H. O. **41:**643–645.
16. **Lucht, E., P. Biberfeld, and A. Linde.** 1995. Epstein-Barr virus (EBV) DNA in saliva and EBV serology of HIV-1-infected persons with and without hairy leukoplakia. J. Infect. **31:**189–194.
17. **Marshall, D. R., S. J. Turner, G. T. Belz, S. Wingo, S. Andreansky, M. Y. Sangster, J. M. Riberdy, T. Liu, M. Tan, and P. C. Doherty.** 2001. Measuring the diaspora for virus-specific $CD8^+$ T cells. Proc. Natl. Acad. Sci. USA **98:**6313–6318.
18. **McMichael, A. J., and C. A. O'Callaghan.** 1998. A new look at T cells. J. Exp. Med. **187:**1367–1371
19. **McNally, J. M., C. C. Zarozinski, M. Y. Lin, M. A. Brehm, H. D. Chen, and R. M. Welsh.** 2001. Attrition of bystander CD8 T cells during virus-induced T-cell and interferon responses. J. Virol. **75:**5965–5976.
20. **Murali-Krishna, K,. J. D. Altman, M. Suresh, D. J. Sourdive, A. J. Zajac, J. D. Miller, J. Slansky, and R. Ahmed.** 1998. Counting antigen-specific CD8 T cells: a reevaluation of bystander activation during viral infection. Immunity **8:**177–187.
21. **Nash, A. A., B. M. Dutia, J. P. Stewart, and A. J. Davison.** 2001. Natural

history of murine γ-herpesvirus infection. Phil. Trans. R. Soc. London B Biol. Sci. **356:**569–579.
22. **Selin, L. K., M. Y. Lin, K. A. Kraemer, D. M. Pardoll, J. P. Schneck, S. M. Varga, P. A. Santolucito, A. K. Pinto, and R. M. Welsh.** 1999. Attrition of T-cell memory: selective loss of LCMV epitope-specific memory CD8 T cells following infections with heterologous viruses. Immunity **11:**733–742.
23. **Speck, S. H., and H. W. Virgin.** 1999. Host and viral genetics of chronic infection: a mouse model of γ-herpesvirus pathogenesis. Curr. Opin. Microbiol. **2:**403–409.
24. **Stevenson, P. G., G. T. Belz, J. D. Altman, and P. C. Doherty.** 1999. Changing patterns of dominance in the CD8+ T-cell response during acute and persistent murine gamma-herpesvirus infection. Eur. J. Immunol. **29:**1059–1067.
25. **Stevenson, P. G., G. T. Belz, M. R. Castrucci, J. D. Altman, and P. C. Doherty.** 1999. A γ-herpesvirus sneaks through a CD8+ T-cell response primed to a lytic-phase epitope. Proc. Natl. Acad. Sci. USA **96:**9281–9286.
26. **Tough, D. F., X. Zhang, and J. Sprent.** 2001. An IFN-γ-dependent pathway controls stimulation of memory phenotype CD8+ T-cell turnover in vivo by interleukin-12, interleukin-18, and IFN-gamma. J. Immunol. **166:**6007–6011.
27. **Townsend, A. R., J. Rothbard, F. M. Gotch, G. Bahadur, D. Wraith, and A. J. McMichael.** 1986. The epitopes of influenza virus nucleoprotein recognized by cytotoxic T lymphocytes can be defined with short synthetic peptides. Cell **44:**959–968.
28. **Tripp, R. A., A. M. Hamilton-Easton, R. D. Cardin, P. Nguyen, F. G. Behm, D. L. Woodland, P. C. Doherty, and M. A. Blackman.** 1997. Pathogenesis of an infectious mononucleosis-like disease induced by a murine γ-herpesvirus: role for a viral superantigen? J. Exp. Med. **185:**1641–1650.
29. **Tripp, R. A., S. Hou, A. McMickle, J. Houston, and P. C. Doherty.** 1995. Recruitment and proliferation of CD8+ T cells in respiratory virus infections. J. Immunol. **154:**6013–6021.
30. **Virgin, H. W., and S. H. Speck.** 1999. Unraveling immunity to γ-herpesviruses: a new model for understanding the role of immunity in chronic virus infection. Curr. Opin. Immunol. **11:**371–379.
31. **Welsh, R. M., J. M. McNally, M. A. Brehm, and L. K. Selin.** 2000. Consequences of cross-reactive and bystander CTL responses during viral infections. Virology **270:**4–8.
32. **Wodarz, D.** 2001. Cytotoxic T-lymphocyte memory, virus clearance and antigenic heterogeneity. Proc. R. Soc. London B Biol. Sci. **268:**429–436.
33. **Wrensch, M., A. Weinberg, J. Wiencke, R. Miike, G. Barger, and K. Kelsey.** 2001. Prevalence of antibodies to four herpesviruses among adults with glioma and controls. Am. J. Epidemiol. **154:**161–165.
34. **Wu, T. T., E. J. Usherwood, J. P. Stewart, A. A. Nash, and R. Sun.** 2000. Rta of murine gammaherpesvirus 68 reactivates the complete lytic cycle from latency. J. Virol. **74:**3659–3667.
35. **Zhang, X., S. Sun, I. Hwang, D. F. Tough, and J. Sprent.** 1998. Potent and selective stimulation of memory-phenotype CD8+ T cells in vivo by interleukin-15. Immunity **8:**591–599.